Eur. Phys. J. B **53**, 455–461 (2006)
DOI: 10.1140/epjb/e2006-00404-6

THE EUROPEAN PHYSICAL JOURNAL B

Spin-polarized transport through a time-periodic non-magnetic semiconductor heterostructure

K. Gnanasekar[1,a] and K. Navaneethakrishnan[2,b]

[1] The American College, Madurai 625002, India
[2] School of Physics, Madurai-Kamaraj University, Madurai 625021, India

Received 8 August 2006 / Received in final form 21 September 2006
Published online 8 November 2006 –

Abstract. Spin-dependent Floquet scattering theory is developed to investigate the photon-assisted spin-polarized electron transport through a semiconductor heterostructure in the presence of an external electric field. Spin-dependent Fano resonances and spin-polarized electron transport through a laser irradiated time-periodic non-magnetic heterostructure in the presence of Dresselhaus spin-orbit interaction and a gate-controlled Rashba spin-orbit interaction are investigated. The electric field due to laser along with the spin-orbit interactions help to get spin-dependent Fano resonances in the conductance, whereas the external bias can be appropriately adjusted to get a near 80% spin-polarized electron transmission through heterostructures. The resultant nature of the Floquet scattering depends on the relative strength of these two electric fields.

PACS. 85.75.Mm Spin polarized resonant tunnel junctions – 72.20.-i Conductivity phenomena in semiconductors and insulators – 73.40.Gk Tunneling – 73.63.Hs Quantum wells

1 Introduction

Spin polarized transport of electrons in time-periodic mesoscopic systems is a subject of increasing technological importance in the growing field of spintronics. Photon-assisted transport has been observed in quantum resonant tunneling structures [1] such as quantum dots [2,3], and superlattices [4]. Quantum interference between a bound state and the continuum of band in time-periodic mesoscopic system leads to Fano-type resonances. First tunable Fano resonances were observed experimentally [5] in a mesoscopic system, realized in an Aharonov-Bohm ring with a quantum dot embedded in one of its arms. Recently, Fano-type resonances due to the interaction of electron states with opposite spin orientation in Datta and Das spin modulators were reported [6] and the splitting of Fano resonances due to Dresselhaus spin-orbit interaction was investigated [7]. Understanding this type of spin-dependent phenomenon may find applications in designing high-speed switching spintronic devices and high-frequency radiation sources and detectors.

In the present work we generalize the model given in reference [7] to investigate the spin dependent Fano resonances and spin-polarized electron transport through a dynamically driven heterostructure due to laser irradiation in the presence of a gate-controlled spin-orbit interaction. Gate-controlled spin degree of freedom is of great importance in the prospects of technological applications of spintronics [8–10]. Gate-controlled Rashba spin-orbit interaction was recently demonstrated experimentally for both electrons and holes in various materials [11–14]. We consider the interferometer geometry which is realized by a laser irradiated quantum well in non-magnetic semiconductor heterostructure. Along with the Dresselhaus spin-orbit interaction, a gate-controlled Rashba spin-orbit interaction is also included in our investigation of spin-dependent Fano resonances and spin-polarized electron transport through such a heterostructure. In our geometry, laser is irradiated such that the electric field due to laser and the externally applied electric field which is used to tune the Rashba spin-orbit interaction are mutually perpendicular to each other. The resultant nature of the Floquet scattering depends on the relative strength of these two electric fields. The electric field due to laser helps to get Fano-type resonances in the conductance, whereas the external bias can be appropriately adjusted to get a near 80% spin-polarized electron transmission through heterostructures. The same model can be used for the case where the two electric fields are parallel and along the growth direction by dividing the time-periodic region into many smaller regions such that the electric potential due laser is constant but different in every such smaller regions.

In Section 2 we elaborate the model which is used to investigate the Fano resonances and spin-polarized transport of electrons through a time-periodic heterostructure

[a] e-mail: kgnnskr@yahoo.com
[b] e-mail: drknk2003@yahoo.co.in

in the presence of a gate-controlled spin-orbit interaction. In Section 3 we study the behavior of Fano resonances, spin dependent transmission probabilities, spin polarization, and spin polarized conductance in a laser irradiated quantum well of GaSb, sandwiched between the layers of InP heterostructure, in the presence of Dresselhaus spin-orbit interaction and a gate-controlled Rashba spin-orbit interaction. In Section 4 we make some concluding remarks.

2 Model and formalism

We consider the spin-dependent transmission of an electron with incident wave vector $\vec{k} = (k_\parallel \cos\phi, k_\parallel \sin\phi, k_z)$, ϕ is the angle of the wave vector $\vec{k}$ in the xy plane, through a laser-irradiated quantum well of InP-GaSb-InP 3-layer non-magnetic semiconductor heterostructure with $z \parallel [001]$ as the growth axis. The electron motion through such a heterostructure in the presence of external electric field, $\vec{F}$, applied along the growth axis is described by the Schrödinger equation:

$$i\hbar\frac{\partial}{\partial t}\Psi_\sigma(\vec{r},t) = \hat{H}\Psi_\sigma(\vec{r},t) \tag{1}$$

with

$$\hat{H}_\sigma = -\frac{\hbar^2}{2\mu}\frac{\partial^2}{\partial z^2} + \frac{\hbar^2 k_\parallel^2}{2\mu} + V(z,t) + H_D - eF(z-z_1) - \sigma\alpha k_\parallel. \tag{2}$$

The potential profile of a harmonically driven heterostructure due to laser field is described by

$$V(z,t) = \begin{cases} -V_0 + V_1\cos\omega t, & 0 \le z \le L \\ 0, & z < 0 \text{ and } z > L. \end{cases} \tag{3}$$

Here V_0 is the depth of the quantum well with width L and which can be harmonically tuned by laser irradiation, as shown in Figure 1. We assume that the quantum well layer is irradiated by laser, such that the potential generated by laser is $eF_l x\cos\omega t$. Here $eF_l x$ is taken as V_1 with F_l, the magnitude of the electric field due to laser. H_D is the spin-dependent k^3 Dresselhaus term that describes the spin-orbit interaction of the semiconductors with zinc-blende lattice structure. For the incident electron with kinetic energy much smaller than the well depth V_0 the Dresselhaus term H_D may be simplified to [15]

$$H_D = \gamma(\sigma_x k_x - \sigma_y k_y)\frac{\partial^2}{\partial z^2} \tag{4}$$

where γ is the material constant describing the strength of the spin-orbit interaction and σ_x and σ_y are the Pauli spin matrices The last two terms in equation (2) are due to external electric field, the last term is the electric field induced Rashba spin-orbit interaction with $\sigma = \pm 1$ corresponds to spin up and spin down respectively and α as the electric field dependent Rashba spin-orbit interaction parameter derived using eight-band $\mathbf{k}\cdot\mathbf{p}$ Kane model [16]:

$$\alpha = \frac{\hbar^2}{2\mu}\frac{\Delta}{E_g}\frac{2E_g + \Delta}{(E_g+\Delta)(3E_g+2\Delta)}eF. \tag{5}$$

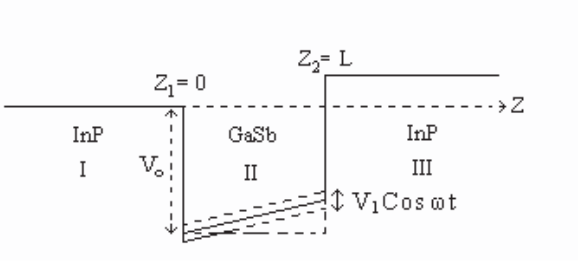

Fig. 1. Potential profile of the non-magnetic semiconductor, InP–GaSb–InP, heterostructure in the presence of laser propagation and the external electric field both along the growth axis (Z-axis). Potential due to laser is $V_1\cos\omega t$, where $V_1 = eF_l x$, which is constant along z-axis.

Here μ is the effective mass of the electron. E_g and Δ are the main band gap and the spin-orbit splitting, respectively. F is the strength of the external electric field. We use a single-electron model at low enough temperatures such that the electron-electron interactions and the electron-phonon interactions can be neglected.

On diagonalizing the Dresselhaus term given in equation (4) by the spinors

$$\chi_\sigma = \frac{1}{\sqrt{2}}\begin{pmatrix} 1 \\ -\sigma e^{-i\phi} \end{pmatrix} \tag{6}$$

which describe the electron spin states with $\sigma = \pm 1$ corresponding to spin up and spin down states respectively. Here ϕ is the angle of the wave vector $\vec{k}$ in the xy plane, $\vec{k}_\parallel = (k_\parallel\cos\phi, k_\parallel\sin\phi)$. One can see that the Dresselhaus spin-orbit interaction modifies the effective mass of the electron as a spin dependent term as given by [17]

$$\mu_\sigma = \mu\left(1 + \frac{2\sigma\gamma\mu k_\parallel}{\hbar^2}\right)^{-1}. \tag{7}$$

Thus the spin dependent Hamiltonian is given by

$$\hat{H}_\sigma = -\frac{\hbar^2}{2\mu_\sigma}\frac{\partial^2}{\partial z^2} + \frac{\hbar^2 k_\parallel^2}{2\mu} + V(z,t) - eF(z-z_0) - \sigma\alpha k_\parallel. \tag{8}$$

2.1 Floquet scattering

The spin-dependent photon-assisted electron transmission through a heterostructure with external bias is described by the Schrödinger equation

$$i\hbar\frac{\partial}{\partial t}\Psi_\sigma(\vec{r},t) = \hat{H}_\sigma\Psi_\sigma(\vec{r},t) \tag{9}$$

with

$$\Psi_\sigma(\vec{r},t) = \chi_\sigma\Phi_\sigma(z,t)e^{i\vec{k}_\parallel\cdot\vec{p}} \tag{10}$$

where $\vec{p} = (x,y)$ is the in-plane vector. Since the potential is time-periodic inside the quantum well, the Floquet theorem [18–20] gives the scattering states

$$\Psi_\sigma^F(\vec{r},t) = \chi_\sigma\Phi_\sigma(z,t)e^{-\frac{iE_F^\sigma t}{\hbar}}e^{i\vec{k}_\parallel\cdot\vec{p}} \tag{11}$$

where E_F is the Floquet eigenenergy and $\phi_\sigma(z,t)$ is a time periodic function: $\phi_\sigma(z,t) = \phi_\sigma(z,t+T)$, with period $T = 2\pi/\omega$. Using equations (10) and (11) along with $\phi_\sigma(z,t) = g_\sigma(z) f_\sigma(t)$, equation (9) separates into following equations:

$$-\frac{\hbar^2}{2\mu_\sigma}\frac{d^2}{dz^2}g_\sigma(z) = \left(E^\sigma + V_0 - \frac{\hbar^2 k_\parallel^2}{2\mu} + eF(z-z_0) + \sigma\alpha k_\parallel\right) g_\sigma(z), \quad (12)$$

$$i\hbar\frac{d}{dt}f_\sigma(t) - V_1\cos\omega t f_\sigma(t) = (E^\sigma - E_F^\sigma) f_\sigma(t), \quad (13)$$

where E^σ is a constant. On integrating equation (13), we get

$$f_\sigma(t) = e^{-i(E^\sigma - E_F^\sigma)t/\hbar}\exp\left[-\frac{i}{\hbar}\int_0^t V_1\cos\omega\tau d\tau\right] = e^{-i(E^\sigma - E_F^\sigma)t/\hbar}\sum_{n=-\infty}^{\infty} J_n\left(\frac{V_1}{\hbar\omega}\right)e^{-in\omega t} \quad (14)$$

with initial condition $f_\sigma(0) = 1$. $J_n(x)$ is the nth order Bessel function of the first kind. Since $f_\sigma(t)$ is periodic, equation (14) requires that $E^\sigma = E_m^\sigma = E_F^\sigma + m\hbar\omega$, where m is an integer.

Since electrons transmitting through the time-periodic region (region II in Fig. 1) will be scattered inelastically into Floquet sidebands with spacing $\hbar\omega$ of energy $E_m^\sigma = E_F^\sigma + m\hbar\omega$ (m is the sideband index), the solution of equation (12) has a form

$$g_\sigma(z) = \sum_{m=-\infty}^{\infty}\{a_{m\sigma}Ai\left[Z_{m\sigma}(z)\right] + b_{m\sigma}Bi\left[Z_{m\sigma}(z)\right]\} \quad (15)$$

where $\{a_{m\sigma}, b_{m\sigma}\}$ are constant coefficients. $Ai\left[Z_{m\sigma}(z)\right]$ and $Bi\left[Z_{m\sigma}(z)\right]$ are Airy functions with

$$Z_{m\sigma}(z) = \left[\frac{2e\mu_\sigma/F/}{\hbar^2}\right]^{\frac{1}{3}}\left[\frac{A_{m\sigma}(E_z) - zeF}{e/F/}\right]$$

and

$$A_{m\sigma}(E_z) = \frac{\hbar^2 k_\parallel^2}{2\mu}\left(1 - \frac{\mu}{\mu_1}\right) - V_0 - E_z - m\hbar\omega - \sigma\alpha k_\parallel + z_1 eF \quad (16)$$

where μ_1 is the effective mass of an electron in region I. Thus the Floquet states in the time-periodic region can be expressed as

$$\Psi_\sigma^{II}(\vec{\rho}, z, t) = \chi_\sigma\sum_{n=-\infty}^{\infty}\sum_{m=-\infty}^{\infty}\{a_{m\sigma}Ai\left[Z_{m\sigma}(z)\right] + b_{m\sigma}Bi\left[Z_{m\sigma}(z)\right]\} \times J_{n-m}\left(\frac{V_1}{\hbar\omega}\right)e^{-iE_{zn}^\sigma t/\hbar}\exp\left(i\vec{k}_\parallel\cdot\vec{\rho} - iE_\parallel^\sigma t/\hbar\right) \quad (17)$$

where E_z is incident energy of the electron and E_{zn}^σ are the Floquet's spin-dependent eigen energies.

2.2 Floquet states outside the time-periodic potential regions

Since electrons incident into the time-periodic potential region will be scattered inelastically into an infinite number of Floquet sidebands, the Floquet states outside the time-periodic regions (i.e. regions I and III in Fig. 1) are the superpositions of an infinite number of plane waves with wave vectors.
For region I

$$k_{1zn}^\sigma = \sqrt{\frac{2\mu_1}{\hbar^2}(E_z^\sigma + n\hbar\omega)} \quad \text{and}$$

for region III

$$k_{3zn}^\sigma = \sqrt{\frac{2\mu_1}{\hbar^2}(E_z^\sigma + n\hbar\omega + eFL)} \quad (18)$$

where is $E_z^\sigma \in [0, \hbar\omega]$ the lowest Floquet energy of the propagating mode. Thus the wave function in regions I and III can be expressed as

$$\Psi_\sigma^I(\vec{\rho}, z, t) = \chi_\sigma\left[e^{ik_{1z0}^\sigma z - iE_{z0}^\sigma t/\hbar} + \sum_{n=-\infty}^{\infty} r_{n0}^\sigma e^{-ik_{1zn}^\sigma z - iE_{zn}^\sigma t/\hbar}\right]e^{i\vec{k}_\parallel\cdot\vec{\rho} - iE_\parallel t/\hbar} \quad (19)$$

and

$$\Psi_\sigma^{III}(\vec{\rho}, z, t) = \chi_\sigma\sum_{n=-\infty}^{\infty} t_{n0}^\sigma e^{ik_{3zn}^\sigma z - iE_{zn}^\sigma t/\hbar}e^{i\vec{k}_\parallel\cdot\vec{\rho} - iE_\parallel t/\hbar} \quad (20)$$

where r_{n0}^σ and t_{n0}^σ are the probability amplitudes of reflecting and transmitting waves from the sideband 0 to sideband n, respectively.

2.3 Conductance of the electrons and spin-polarization

Across the interfaces between different layers the wave function Ψ_σ and the flux $\frac{1}{\mu}\frac{\partial}{\partial z}\Psi_\sigma$ have to be continuous. Here the contribution to Rashba spin-orbit interaction due to band bending is neglected, as its contribution to transport is negligibly smallcompared to the contribution from external electric field [21]. At the interface between layers I and II, since $z = 0$, these conditions lead to

$$\sum_{m=-\infty}^{\infty} J_{n-m}\left(\frac{V_1}{\hbar\omega}\right)\{a_{m\sigma}Ai\left[Z_{m\sigma}(0)\right] + b_{m\sigma}Bi\left[Z_{m\sigma}(0)\right]\} = \delta_{n0} + r_{n0}^\sigma, \quad (21)$$

$$\frac{\mu_1}{\mu_\sigma}\sum_{m=-\infty}^{\infty} J_{n-m}\left(\frac{V_1}{\hbar\omega}\right)\left\{a_{m\sigma}\frac{\partial}{\partial z}Ai\left[Z_{m\sigma}(z)\right]\Big|_{z=0} + b_{m\sigma}\frac{\partial}{\partial z}Bi\left[Z_{m\sigma}(z)\right]\Big|_{z=0}\right\} = ik_{1zn}^\sigma\left(\delta_{n0} + r_{n0}^\sigma\right). \quad (22)$$

At the interface between layers II and III, since $z = L$,

$$\sum_{m=-\infty}^{\infty} J_{n-m}\left(\frac{V_1}{\hbar\omega}\right)\{a_{m\sigma}Ai\left[Z_{m\sigma}(L)\right] + b_{m\sigma}Bi\left[Z_{m\sigma}(L)\right]\} = e^{ik^{\sigma}_{3zn}L}t^{\sigma}_{n0}, \quad (23)$$

$$\frac{\mu_1}{\mu_\sigma}\sum_{m=-\infty}^{\infty} J_{n-m}\left(\frac{V_1}{\hbar\omega}\right)\left\{a_{m\sigma}\frac{\partial}{\partial z}Ai\left[Z_{m\sigma}(z)\right]\Big|_{z=L} + b_{m\sigma}\frac{\partial}{\partial z}Bi\left[Z_{m\sigma}(z)\right]\Big|_{z=L}\right\} = ik^{\sigma}_{3zn}\left(e^{ik^{\sigma}_{3zn}L}t^{\sigma}_{n0}\right). \quad (24)$$

The continuity conditions (21–24) can be expressed in matrix form:

$$\boldsymbol{J}(\boldsymbol{CA} + \boldsymbol{DB}) = \Delta + \boldsymbol{R} \quad (25)$$

$$\frac{\mu_1}{\mu_\sigma}\boldsymbol{J}(\Omega\boldsymbol{A} + \Lambda\boldsymbol{B}) = \boldsymbol{K}(\Delta - \boldsymbol{R}) \quad (26)$$

$$\boldsymbol{J}(\boldsymbol{GA} + \boldsymbol{PB}) = \boldsymbol{ST} \quad (27)$$

$$\frac{\mu_1}{\mu_\sigma}\boldsymbol{J}(\boldsymbol{QA} + \boldsymbol{LB}) = \Gamma\boldsymbol{ST} \quad (28)$$

with the square matrices defined by $\boldsymbol{C_{nm}} = \boldsymbol{Ai}[\boldsymbol{Z_{m\sigma}}(0)]\delta_{\boldsymbol{nm}}$, $\boldsymbol{D_{nm}} = \boldsymbol{Bi}[\boldsymbol{Z_{m\sigma}}(0)]\delta_{\boldsymbol{nm}}$, $G_{nm} = Ai[Z_{m\sigma}(L)]\delta_{nm}$, $P_{nm} = Bi[Z_{m\sigma}(L)]\delta_{nm}$, $\Omega_{nm} = \frac{\partial}{\partial z}Ai[Z_{m\sigma}(z)]\Big|_{z=0}\delta_{nm}$, $\Lambda_{nm} = \frac{\partial}{\partial z}Bi[Z_{m\sigma}(z)]\Big|_{z=0}\delta_{nm}$, $Q_{nm} = \frac{\partial}{\partial z}Ai[Z_{m\sigma}(z)]\Big|_{z=L}\delta_{nm}$, $L_{nm} = \frac{\partial}{\partial z} \times Bi[Z_{m\sigma}(z)]\Big|_{z=L}\delta_{nm}$, $S_{nm} = e^{ik^{\sigma}_{3zn}L}\delta_{nm}$, $K_{nm} = ik^{\sigma}_{1zn}\delta_{nm}$, $\Gamma_{nm} = ik^{\sigma}_{3zn}\delta_{nm}$ and column matrices $\boldsymbol{A_n} = \boldsymbol{a_{n\sigma}}$, $\boldsymbol{B_n} = \boldsymbol{b_{n\sigma}}$, $\boldsymbol{\Delta_n} = \delta_{\boldsymbol{n0}}$, $\boldsymbol{R_n} = \boldsymbol{r^{\sigma}_{n0}}$, $\boldsymbol{T_n} = \boldsymbol{t^{\sigma}_{n0}}$. Here $\boldsymbol{R}$ and $\boldsymbol{T}$ denote the matrices of reflection and transmission amplitudes. Solving matrix equations (25–28), we obtain the matrix of transmission amplitude:

$$\boldsymbol{T} = 2\boldsymbol{S}^{-1}\left[(\boldsymbol{KJC} + \boldsymbol{J}\Omega)\boldsymbol{M}_1^{-1}\boldsymbol{M}_3 + (\boldsymbol{KJD} + \boldsymbol{J}\Lambda)\boldsymbol{M}_2^{-1}\boldsymbol{M}_4\right]^{-1}\boldsymbol{K}\Delta \quad (29)$$

where $\boldsymbol{M}_1 = \left[\boldsymbol{JLP}^{-1}\boldsymbol{G} - \boldsymbol{JQ}\right]$, $\boldsymbol{M}_2 = \left[\boldsymbol{JQG}^{-1}\boldsymbol{P} - \boldsymbol{JL}\right]$, $\boldsymbol{M}_3 = \left[\boldsymbol{JLP}^{-1}\boldsymbol{J}^{-1} - \frac{\mu_\sigma}{\mu_1}\Gamma\right]$, and $\boldsymbol{M}_4 = \left[\boldsymbol{JQG}^{-1}\boldsymbol{J}^{-1} - \frac{\mu_\sigma}{\mu_1}\Gamma\right]$. The total electron transmission probabilities of spin-up and spin-down components are given by

$$T^{\sigma} = \sum_{m=0}^{\infty}|t^{\sigma}_{m0}|^2 \quad (30)$$

from which the spin-polarized conductance of the electrons through a time-periodic semiconductor heterostructures can be obtained by the Landauer-Buttiker formula [22,23]

$$G^{\sigma} = \frac{e^2}{h}T^{\sigma}. \quad (31)$$

The spin polarization efficiency of the transmitted electron can be found from

$$P_s = \frac{T^{+1} - T^{-1}}{T^{+1} + T^{-1}}. \quad (32)$$

3 Results and discussion

We have investigated the effect of a gate-controlled Rashba spin-orbit interaction and Dresselhaus spin-orbit interaction on the Fano resonance and spin-polarized electron transport through a laser irradiated InP–GaSb–InP non-magnetic semiconductor heterostructure. Laser is irradiated and the external electric field is applied to the quantum well region along the growth axis, so that the electric field due laser and the external electric field are mutually perpendicular. Spin-dependent conductance and the spin-polarization efficiency are calculated as a function of incident electron energy and spin, using equations (31) and (32). The number of sidebands, N, included in the calculation of transmission probability, given in equation (30), depends on the relative strength of the modulation amplitude of the quantum well and the lowest energy of the propagating mode [24], such that $N > V_1/\hbar\omega$. The material parameters used in our calculations are $\gamma_1 = 187$ eV Å^3, $\mu = 0.041\ m_e$ (m_e is the rest mass of the electron) for GaSb, and $\gamma = 8$ eV Å^3, $\mu_1 = 0.081\ m_e$ for InP as given in references [7,15,16].

In our model, electrons move freely from left to right with energy E_{z0} may get 'scattered' by infinite number of Floquet states, which are due to time-periodic nature of the quantum well. Whenever the incident energy of the electron is equal to an integer multiple of energy of one photon, a photon-assisted transmission resonance occurs. In our calculation of the spin-dependent conductance, we consider a three layer heterostructure InP–GaSb–InP with a quantum well of depth $V_0 = 300$ meV, well width $L = 60$ Å, and $k_{||} = 10^6$ cm^{-1}; also since $\gamma_1 \gg \gamma$, we take $\gamma = 0$.

In Figure 2 we show the Photon-assisted transmission in the presence of external electric field without considering the spin-orbit interactions. Figures 2a and 2b show the conductance as a function of incident energy of electron in the presence of external electric field alone. These graphs show the resonant transmission of electrons and that the number of bound states available for resonant decreases as the strength of the external electric field increases due to tapering of the potential well as shown in Figure 1. Figures 2c and 2d depict conductance in the presence of external electric field through a laser irradiated heterostructure with the laser induced modulating potential $V_1 = 10$ meV, and $\hbar\omega = 10$ meV. Both of them show the Fano-type resonances and the number of occurrence of Fano resonances decreases, because the number of quasi-bound states available for resonance decreases as the strength of the external electric field increases.

Figure 3 shows the shifting of the Fano-type resonance peaks position towards the higher energy region as the modulating frequency increases. It gives an additional degree of freedom to control the location of resonance apart from the parameters of the heterostructure. Figure 3b shows two Fano resonances, around the incident energy $E_z = 5$ meV and $E_z = 10$ meV. Since the magnitude of the second Fano resonance is small, it may correspond to two photon process whose probability of occurrence is small.

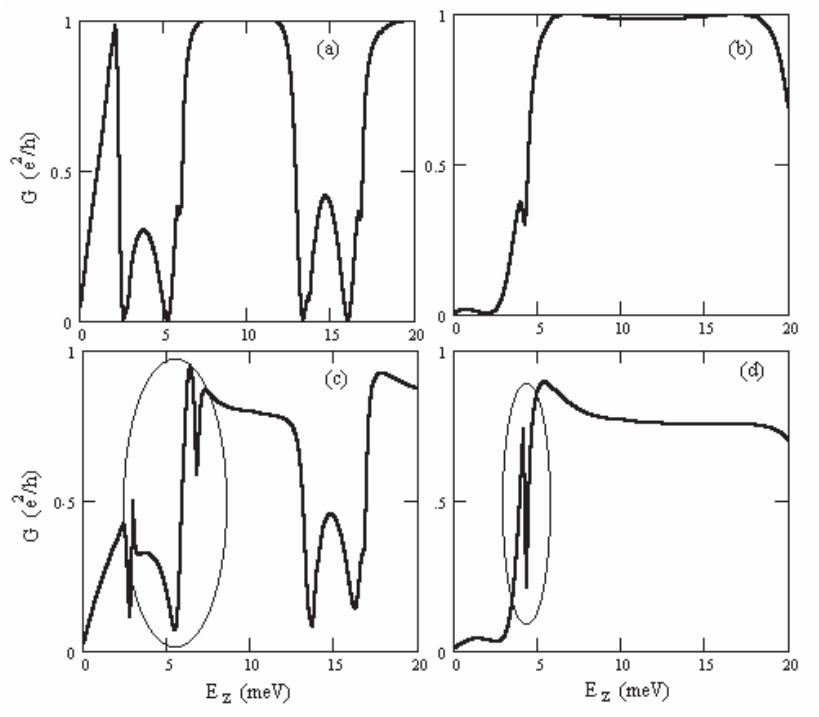

Fig. 2. Conductance as a function of E_z, in the presence of different external electric field but without spin-orbit interactions, for V_0 = 300 meV, L = 60 Å, $k_{||} = 10^6$ cm^{-1}, μ = 0.041 m_e, and μ_1 = 0.081 m_e. (a) and (b) with out laser irradiation, whereas (c) and (d) are with laser irradiation (V_1 = 10 meV, and $\hbar\omega$ = 10 meV). (a) and (c) in the presence of external electric field, $F = 2 \times 10^6$ V/m but (b) and (d) with $F = 5 \times 10^6$ V/m. Fano-type resonances are shown by elliptical markings.

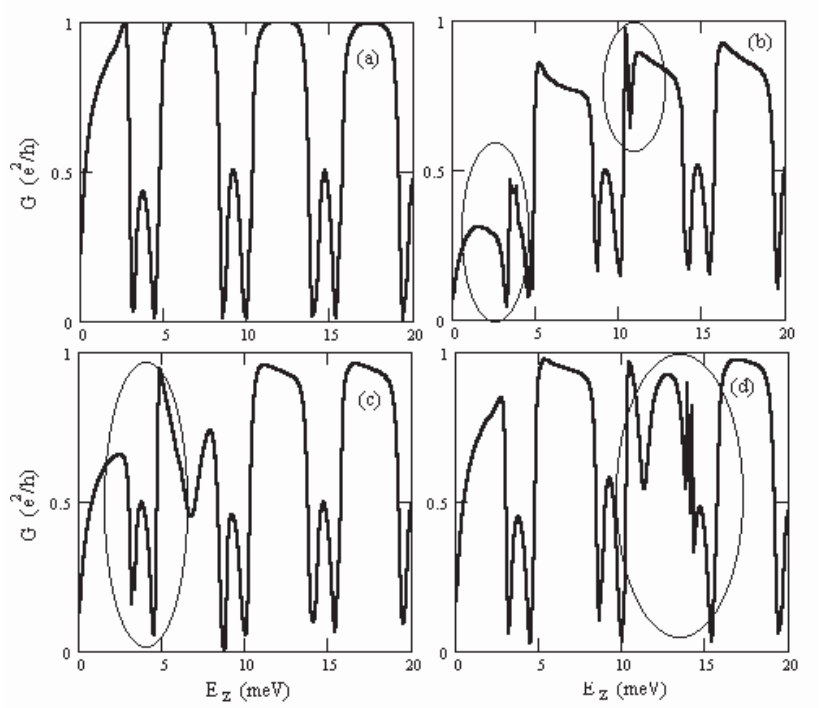

Fig. 3. Conductance as a function of E_z, in the presence of external electric field, $F = 10^6$ V/m but without spin-orbit interactions, for V_0 = 300 meV, L = 60 Å, $k_{||} = 10^6$ cm^{-1}, μ = 0.041 m_e, and μ_1 = 0.081 m_e. (a) without laser irradiation, whereas (b), (c) and (d) are with laser irradiation (V_1 = 10 meV). (b) for $\hbar\omega$ = 10 meV, (c) for $\hbar\omega$ = 15 meV, and (d) for $\hbar\omega$ = 20 meV. Fano-type resonances are shown by elliptical markings. Second elliptical marking in (b) may correspond to two photon Fano resonance.

In Figure 4 we show the effect of external electric field and a gate-controlled spin-orbit interaction on the spin-dependent Fano resonance and the spin-polarized electron transport. Figure 4a shows a set of sharp spin-dependent Fano resonances in the absence of electric field for a range of incident electron energy up to 20 meV, as reported in reference [7] and the other graphs 4b, 4c, and 4d show the effect of external electric field. These graphs show the electrically tunable spin-polarized electron transport with increased transmission. Figure 4d show the non-occurrence of Fano resonance in the energy range of incident energy below 20 meV, even though the strength of modulating potential (V_1 = 10 meV) and frequency ($\hbar\omega$ = 10 meV) are within this range. These graphs show that the nature and location of the Fano-type resonance depends on the relative strength of the electric field due to laser and the external electric field.

Figure 5 shows the variation of Polarization efficiency of the transmission of electrons with energy and spin of the

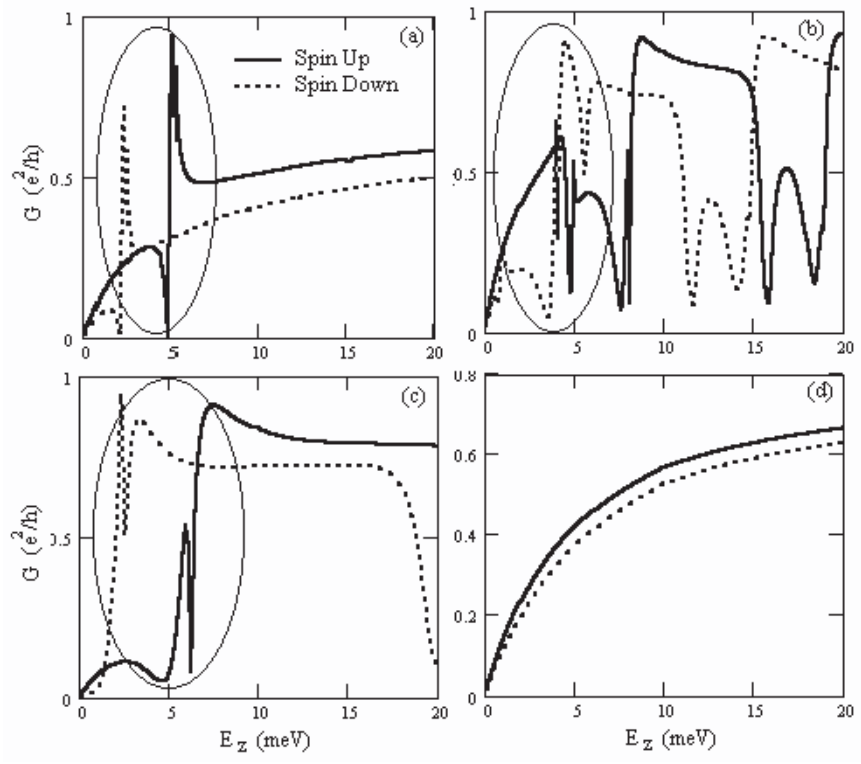

Fig. 4. Conductance G^σ as a function of E_z, in the presence of different external electric field for $V_0 = 300$ meV, $V_1 = 10$ meV, $L = 60$ Å, $k_{||} = 10^6$ cm^{-1}, $\hbar\omega = 10$ meV, $\mu = 0.041\ m_e$, $\mu_1 = 0.081\ m_e$, $\gamma = 187$ eV Å^3, and $\gamma_1 = 0$. (a) for zero-field, (b) for $F = 10^6$ V/m, (c) for $F = 5 \times 10^6$ V/m, (d) for $F = 15 \times 10^6$ V/m. Fano-type resonances are shown by elliptical markings. It shows the increasing transmission probability and the nature of Fano-type resonances with the strength of external electric field.

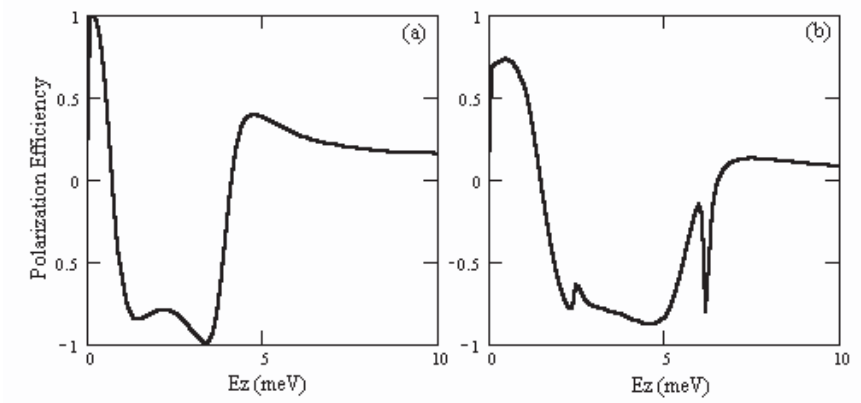

Fig. 5. Variation of Polarization efficiency of the transmission electrons with the energy and spin of the incident electron, in the presence of external electric field. Positive Polarization efficiency corresponds to spin-up electrons and the negative corresponds to spin-down electrons. (a) zero-field case with $V_1 = 30$ meV, (b) for $F = 5 \times 10^6$ V/m with $V_1 = 10$ meV, and the other parameters are the same as in Figure 4.

incident electrons. This shows the possibility of designing a gate-controlled spin filter for the future applications of spintronics.

4 Conclusions

We have developed the spin-dependent Floquet scattering theory of the photon-assisted spin-polarized electron transport through semiconductor heterostructures in the presence of an external electric field. The nature of Fano resonances and the spin-polarized electron transport through a laser irradiated quantum well under external bias with Dresselhaus spin-orbit interaction and a gate-controlled Rashba spin-orbit interaction are investigated using this theory. Our investigations show that (i) the nature of Fano resonance is dependent on the relative strength of the electric field due to laser and the external electric field; (ii) the modulating frequency gives an additional degree of freedom to control the location of resonance apart from the structural parameters of the heterostructure; (iii) enhancement of spin polarization efficiency. These investigations enlighten our fundamental understanding of photon-assisted spin-transport and its related phenomena through non-magnetic semiconductor heterostructure. These features could be appropriately optimized to design an electrically tunable spin filters.

One of us (K.G.) would like to acknowledge the University Grants Commission (UGC), India for a grant under Faculty Development Programme and the American College for permission. We gratefully acknowledge the research support to the School of Physics under DRS by UGC of India.

References

1. R. Tsu, L. Esaki, Appl. Phys. Lett. **22**, 562 (1973)
2. L.P. Kouwenhoven, S. Jauhar, J. Orenstein, P.L. McEuen, Y. Nagamune, J. Motohisa, H. Sakaki, Phys. Rev. Lett. **73**, 3443 (1994)
3. R.H. Blick, R.J. Haug, D.W. van der Weide, K. von Klitzing, K. Eberl, Appl. Phys. Lett. **67**, 3924 (1995)
4. B.J. Keay, S.J. Allen, Jr, J. Galan, J.P. Kaminski, K.L. Campman, A.C. Gossard, U. Bhattacharya, M.J.W. Rodwell, Phys. Rev. Lett. **75**, 4098 (1995); B.J. Keay, S. Zeuner, S.J. Allen, Jr, K.D. Maranowski, A.C. Gossard, U. Bhattacharya, M.J.W. Rodwell, Phys. Rev. Lett. **75**, 4102 (1995)
5. K. Kobayashi, H. Aikawa, S. Katsumoto, Y. Iye, Phys. Rev. Lett. **88**, 256806 (2002)
6. I.A. Shelykh, N.G. Galkin, Phys. Rev. B **70**, 205328 (2004)
7. C.-X. Zhang, Y.-H. Nie, J.-Q. Liang, Phys. Rev. B **73**, 085307 (2006)
8. J.M. Kikkawa, I.P. Smorchkova, N. Samarth , D.D. Awschalom, Science **277**, 1284 (1997); J.P. Morten, A. Brataas, W. Belzig, Phys. Rev. B **72**, 014510 (2005)
9. S. Datta, B. Das, Appl. Phys. Lett. **56**, 665 (1990); D.J. Monsma, R. Vlutters, J.C. Lodder, Science, **281**, 407 (1998)
10. D.P. Divincenzo, Science **270**, 255 (1995); B.E. Kane, Nature (London) **393**, 133 (1998)
11. J. Nitta, T. Akasaki, H. Takayanagi, T. Enoki, Phys. Rev. Lett. **78**, 1335 (1997)
12. J.P. Heida, B.J. van Wees, J.J. Kuipers, T.M. Klapwijk, G. Broghs, Phys. Rev. B **57**, 11911 (1998)
13. G. Engels, J. Lange, Th. Schapers, H. Luth, Phys. Rev. B **55**, R1958 (1997)
14. D. Grundler, Phys. Rev. Lett. **84**, 6074 (2000)
15. V.I. Perel, S.A. Tarasenko, I.N. Yassievich, S.D. Ganichev, V.V. Belkov, W. Prettl, Phys. Rev. B **67**, 201304(R) (2003)
16. E.A. de Andrada e Silva, G.C. La Rocca, F. Bassani, Phys. Rev. B **50**, 8523 (1994); E.A. de Andrada e Silva, G.C. La Rocca, F. Bassani, Phys. Rev. B **55**, 16293 (1997); A. Voskoboynikov, S.S. Liu, C.P. Lee, Phys. Rev. B **59**, 12514 (1999); E.A. de Andrada e Silva, G.C. La Rocca, Phys. Rev. B **59**, 15583 (1999); A. Voskoboynikov, S.S. Liu, C.P. Lee, O. Tretyak, J. Appl. Phys. **87**, 387 (2000)
17. M.M. Glazov, P.S. Alekseev, M.A. Odnoblyudov, V.M. Chistyakov, S.A. Tarasenko, I.N. Yassievich, Phys. Rev. B **71**, 155313 (2005)
18. J.H. Shirley, Phys. Rev. B **138**, 979 (1965)
19. M. Holthaus, D. Hone, Phys. Rev. B **47**, 6499 (1993)
20. T. Fromherz, Phys. Rev. B **56**, 4772 (1997)
21. K. Gnanasekar, K. Navaneethakrishnan, Phys. Lett. A **341**, 495 (2005)
22. R. Landauer, J. Phys.: Condens. Matter **1**, 8099 (1989)
23. M. Buttiker, Phys. Rev. Lett. **57**, 1761 (1986); T. Christen, M. Buttiker, Phys. Rev. Lett. **77**, 143 (1996)
24. E.N. Bulgakov, A.F. Sadreev, J. Phys.: Condens. Matter **8**, 8869 (1996)